Mechanochemistry

DOI: 10.1002/anie.201003978

Competition between Orbitals and Stress in Mechanochemistry**

*Gurpaul S. Kochhar, Adrian Bailey, and Nicholas J. Mosey**

The use of mechanical stress to guide molecular systems along specific reaction pathways has gained considerable interest recently.[1] This interest has been driven by sonication experiments,[2] which showed that the ring opening of benzocyclobutene (BCB) with polymeric substituents on the carbon atoms of the scissile bond can be selectively directed along competing pathways in violation of the Woodward–Hoffmann (WH) rules.[3] Specifically, the thermally allowed conrotatory pathway was followed if the substituents were in a *trans* configuration with respect to the ring, and the thermally forbidden disrotatory pathway was followed if the substituents were in a *cis* configuration. These results were attributed to stress applied across the scissile bond during ultrasound pulses, causing the ring to open along the pathway that moves the polymer substituents farthest apart. Circumventing the WH rules is fundamentally interesting, and more generally, the ability to selectively activate competing reactions with mechanical stress may be of synthetic value.

The mechanochemical ring openings of cyclobutene (CB) and BCB were further investigated using quantum chemical methods.[4,5] These studies confirmed that applying an external force of magnitude F_{ext} can selectively activate the ring opening of CB along controtary or disrotatory pathways based on the location of the atoms used as pulling points (PPs). This was determined on the basis of reaction barriers calculated by treating the system as moving on a force-modified potential energy surface (FMPES) [Eq. (1)]:

$$V(\mathbf{q},F_{ext}) = V_{BO}(\mathbf{q}) - F_{ext}\,x(\mathbf{q}) \quad (1)$$

where $\mathbf{q}$ represents the atomic positions, V_{BO} is the Born–Oppenheimer (BO) potential energy, and $x(\mathbf{q})$ is the distance between the PPs. Pathways along which $x(\mathbf{q})$ increases upon moving from reactant to transition state (TS) will experience a decreased barrier relative to that in the absence of F_{ext}.

The theoretical studies explained the mechanochemical ring opening of CB along the forbidden pathway in terms of energetics. However, the WH rules are ultimately based on orbital symmetries. The typical route taken to follow a thermally forbidden pathway is to irradiate the system, changing the electronic state and orbital occupations. F_{ext} does not interact directly with the electronic structure (ES) in a manner that can induce electronic excitations. Therefore, it would be of fundamental value to determine how applying F_{ext} promotes WH forbidden reactions. Herein, we use quantum chemical methods to study how the ES evolves during the disrotatory ring opening of CB under mechanochemical conditions.

The disrotatory ring opening of CB was investigated by performing molecular dynamics (MD) simulations on the FMPES. CASSCF(4,4)/6-31G(d,p) was used to evaluate V_{BO} and hydrogens on the carbon atoms of the scissile bond were used as PPs, with the PPs in a *cis* configuration to activate the disrotatory process. The simulations showed that the forbidden process occurs when $F_{ext} \geq 2800$ pN. These results are consistent with previous MD simulations except that the minimum value of F_{ext} needed to induce the reaction in this study is approximately twice that reported earlier.[5] This discrepancy may be due to difference in methods.

The populations of the natural orbitals comprising the active space were monitored during the simulations. These populations (Figure 1 a) indicate that the system is closed-shell for the majority of the simulation. A diradical was formed at $t \approx 1.6$ ps, which coincided with the disrotatory ring opening. The diradical is not a stationary point, however it is a structure that the system passes through along the reaction coordinate. Previous calculations have shown that diradical formation occurs during this reaction when $F_{ext} = 0$ pN,[6,7] and is necessary to meet the changes in orbital symmetry that occur during this reaction.[7]

Intrinsic reaction coordinate (IRC) calculations were performed to study the ES over a wider range of F_{ext} than was possible with the MD simulations. The calculated populations along the IRCs are shown in Figure 1 b. All plots show progression through a diradical structure, showing that F_{ext} does not cause the evolution of the ES to differ significantly from $F_{ext} = 0$ pN. This confirms the assertion that applying F_{ext} can activate the forbidden reaction without changing the electronic state.

The separation between the TS and diradical along the reaction coordinate increases with F_{ext}. This implies a change in the geometries of either or both of these structures with F_{ext}. To explore this, we compared the structural details of the TSs and diradicals calculated at different F_{ext} (line structures in Figure 2). It is clear that the TS is more significantly affected by F_{ext}, with this structure shifting toward the reactant as F_{ext} increases. For example, the distance between carbon atoms in the scissile bond of the TS at $F_{ext} = 3000$ pN (2.071 Å) is much shorter than that at $F_{ext} = 0$ pN (2.851 Å). The shift in the position of the TS along the reaction coordinate is consistent with the tilting mechanism proposed previously.[8] More rigorously, this shift reflects the change in the PES with the application of F_{ext}, which alters the reaction

[*] G. S. Kochhar, A. Bailey, Prof. N. J. Mosey
Department of Chemistry, Queen's University
90 Bader Lane, Kingston, ON, K7L 3N6 (Canada)
Fax: (+1) 613-533-6669
E-mail: nicholas.mosey@chem.queensu.ca

[**] This work was funded by the Natural Sciences and Engineering Research Council (NSERC) of Canada. Computing resources were provided by SHARCNET and HPCVL.

Supporting information for this article is available on the WWW under http://dx.doi.org/10.1002/anie.201003978.

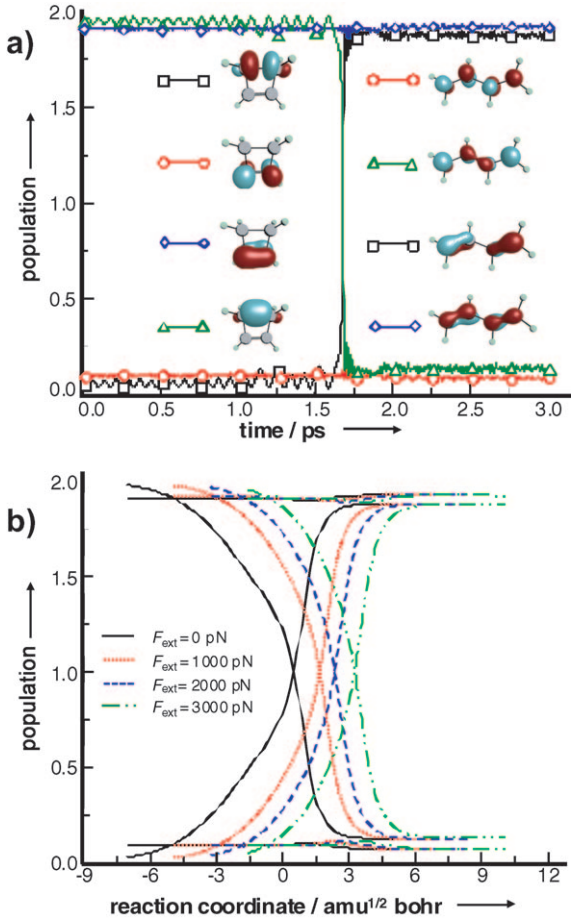

Figure 1. a) Populations of the natural orbitals comprising the active space during the MD simulation with $F_{ext} = 2800$ pN. The orbitals in the reactants and products are shown at the left and right, respectively, and different colored curves denote correlated orbitals. The orbitals are plotted at contour values of 0.1 au, and colors indicate different phases of the wavefunction. The orbitals are arranged from bottom to top in increasing energy. b) Populations of the natural orbitals comprising the active space along the IRCs. The orbitals monitored are analogous to those shown in (a). The transition state is located at 0 amu$^{1/2}$ bohr. Four curves are shown for each F_{ext}.

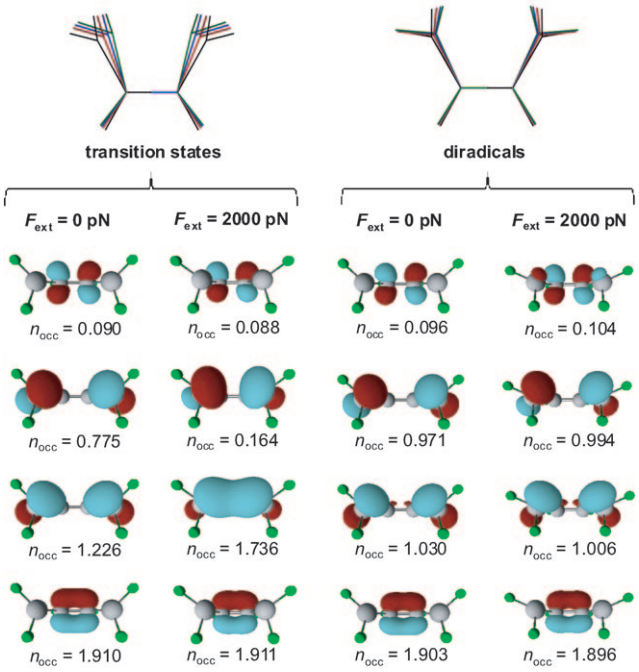

Figure 2. Structures, natural orbitals, and natural orbital populations of the TSs and diradicals along the disrotatory pathway. The line structures provide a comparison of the structures of the TSs and diradicals with black, red, blue, and green lines representing $F_{ext} = 0$, 1000, 2000, and 3000 pN. The natural orbitals comprising the active space of the TSs and diradicals evaluated with $F_{ext} = 0$ and 2000 pN are shown below the line structures along with their populations. The orbitals are plotted at a contour value of 0.1 au. Different colors of the orbitals indicate different phases of the wavefunction.

pathway itself.[4] Meanwhile, the diradicals all exhibit similar structures regardless of F_{ext}. This is not surprising because the ES is determined by geometry, and there exists a limited set of structures on the BO surface whose ground state wavefunction correponds to a diradical.

The shift in the position of the TS is also evident from the orbitals plotted in Figure 2. A comparison of the TS at $F_{ext} = 0$ and 2000 pN shows that the latter has significant σ bonding character between the atoms in the scissile bond, while the former does not. The orbital populations in the TS at $F_{ext} = 0$ pN indicate that the TS has a high degree of diradical character. Meanwhile, the orbital populations in the TS at $F_{ext} = 2000$ pN are closer to 0 and 2, indicating that this structure is shifted toward the reactant. This is consistent with the interpretation above.

The shift in the position of the TS toward the reactant with increasing F_{ext} causes the TS and reactant to have increasingly similar structures, and hence energies, reducing the barrier with F_{ext} (Supporting Information). However, the results also show that diradical formation occurs regardless of F_{ext}. The changes in orbital structures and populations leading to diradical formation are disfavored on the ground state. Furthermore, applying F_{ext} cannot change the electronic state, and must instead induce the necessary changes in ES by altering the geometry on the ground-state PES.

To investigate how F_{ext} drives the forbidden reaction on the ground state PES, we expand Equation (1) as:

$$E = \left\langle \Psi \left| -\frac{\nabla^2}{2} - \sum_{I=1}^{M}\sum_{i=1}^{N}\frac{Z_I}{r_{iI}} + \sum_{i=1}^{N-1}\sum_{j>i}^{N}\frac{1}{r_{iI}} \right| \Psi \right\rangle + \sum_{I=1}^{M-1}\sum_{J>I}^{M}\frac{Z_I Z_J}{r_{IJ}} - F_{ext}x \qquad (2)$$

to explicitly show the contributions from the electronic energy (E_{elec}), nuclear–nuclear repulsion (E_{NN}) and mechanical work (E_{mech}), which correspond to the first, second and third terms on the right-hand side, respectively. Note that in Equation (2) atomic units have been used, Ψ is the electronic wavefunction, M and N are the number of nuclei and electrons, respectively, Z_I is the charge of nucleus I, and r_{ij}, r_{Ii} and r_{IJ} correspond to electron–electron, electron–nucleus, and nucleus–nucleus distances, respectively.

Differentiating each term in Equation (2) with respect to the reaction coordinate, **s**, yields an effective force, $\tilde{\mathbf{F}}_k = -\nabla_s E_k$, corresponding to how each energy contribution affects the motion of the system along the reaction coordinate, where k indicates whether the derivative is evaluated using E_{elec}, E_{NN}, or E_{mech}. Note that $\tilde{\mathbf{F}}_k$ has units of N amu$^{-1/2}$ and is not strictly a force. The relative magnitudes of $\tilde{\mathbf{F}}_k$ determine which factors govern the behavior of the system. $|\tilde{\mathbf{F}}_{elec}| - |\tilde{\mathbf{F}}_{NN} + \tilde{\mathbf{F}}_{mech}|$ and $|\tilde{\mathbf{F}}_{mech}| - |\tilde{\mathbf{F}}_{NN} + \tilde{\mathbf{F}}_{elec}|$ were evaluated along the IRCs calculated at $F_{ext} = 0$, 1000, 2000, and 3000 pN. The first of these quantities compares the electronic factors to all other contributions, while the second compares the mechanical work against all other contributions. Values obtained at $F_{ext} = 0$ and 2000 pN are shown in Figure 3.

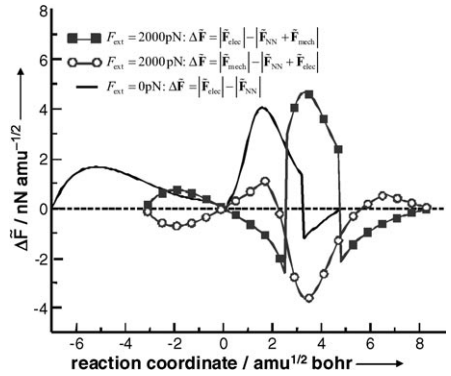

Figure 3. Comparison of contributions to $\tilde{\mathbf{F}}$ from E_{elec}, E_{NN}, and E_{mech} at values of $F_{ext} = 0$ and 2000 pN.

The data in Figure 3 obtained at $F_{ext} = 0$ pN only correspond to $|\tilde{\mathbf{F}}_{elec}| - |\tilde{\mathbf{F}}_{NN}|$ because no work was performed on the system. At this value of F_{ext}, the reactants, TS, and diradical are at positions of −7.0, 0.0, and 0.5 amu$^{1/2}$bohr along the reaction coordinate, respectively. $|\tilde{\mathbf{F}}_{elec}| - |\tilde{\mathbf{F}}_{NN}| \geq 0$ within this region, which indicates that progress of the system from the reactant through the TS and to the diradical is governed by the electronic structure when $F_{ext} = 0$ pN, as opposed to nuclear–nuclear repulsion. This is consistent with the WH rules that classify this process as forbidden on the basis of orbital symmetry.

When $F_{ext} = 2000$ pN, the reactants, TS, and diradical are located at −3.2, 0.0, and 2.4 amu$^{1/2}$bohr along the reaction coordinate, respectively. $|\tilde{\mathbf{F}}_{elec}| - |\tilde{\mathbf{F}}_{NN} + \tilde{\mathbf{F}}_{mech}| > 0$ between the reactants and TS, and drops below 0 between the TS and diradical. Similarly, $|\tilde{\mathbf{F}}_{mech}| - |\tilde{\mathbf{F}}_{NN} + \tilde{\mathbf{F}}_{elec}| < 0$ between the reactants and TS, and exceeds 0 between the TS and diradical. Altogether, this indicates that the BO energy terms ($E_{elec} + E_{NN}$) govern the behavior of the system between the reactant and TS, while mechanical work controls the behavior between the TS and diradical. This illustrates how the system can form the disfavored diradical structure under mechanochemical conditions. Essentially, the electronic factors (and hence the WH rules) that disfavor diradical formation are rendered secondary to mechanochemical effects that favor an increase in $x(\mathbf{q})$ through C–C bond scission in the region of the reaction coordinate between the TS and diradical. These effects were also observed along the IRCs calculated at $F_{ext} =$ 1000 and 3000 pN.

As a whole, the results clarify how reactions forbidden by the WH rules become allowed mechanochemically. The circumvention of the WH rules is not due to a change in ES analogous to that achieved through irradiation. Instead, F_{ext} facilitates these reactions in two ways. First, the application of F_{ext} shifts the TS along the IRC toward the reactants, reducing the reaction barrier. Second, when F_{ext} is applied, the orbital effects that disfavor movement from reactants to products are rendered secondary to mechanochemical factors that favor progression toward products. This notion is supported by calculations of other pericyclic reactions (Supporting Information). The conclusion that F_{ext} does not significantly alter how the ES evolves during a reaction, yet alters the factors that govern the motion of the system at key points along the reaction coordinate likely applies in a broader context, as opposed to the narrow field of pericyclic reactions. As such, this work may be of general value in the practical application of mechanochemistry to other cases where reactions are selectively activated along competing pathways, while retaining the underlying changes in ES that occur along those pathways.

Experimental Section

All geometry optimizations, IRC calculations, and MD simulations were performed with a version of the GAMESS-US software package[9] that we modified to enable calculations on the force-modified potential energy surface. All calculations were performed at the CASSCF(4,4)/6-31G(d,p) level. MD simulations were performed under NVT conditions using a Nose–Hoover thermostat[10] to maintain the temperature at 300 K. A time step of 1.0 fs was used in the MD simulations, which was sufficient to conserve the total energy to 1.0×10^{-5} au ps^{-1} or better.

Received: June 30, 2010
Published online: September 2, 2010

Keywords: computational chemistry · mechanochemistry · pericyclic reactions · Woodward–Hoffmann rules

[1] a) Q.-Z. Yang, Z. Huang, T. J. Kucharski, D. Khvostichenko, J. Chen, R. Boulatov, *Nat. Nanotechnol.* **2009**, *4*, 302 – 306; b) M. Konôpka, R. Turanský, J. Reichert, H. Fuchs, D. Marx, I. Štich, *Phys. Rev. Lett.* **2008**, *100*, 115503; c) S. S. Sheiko, F. C. Sun, A. Randall, D. Shirvanyants, M. Rubinstein, H. Lee, K. Matyjaszewski, *Nature* **2006**, *440*, 191 – 194; d) M. K. Beyer, H. Clausen-Schaumann, *Chem. Rev.* **2005**, *105*, 2921 – 2948.
[2] C.R Hickenboth, J. S. Moore, S. R. White, N. R. Sottos, J. Baudry, S. R. Wilson, *Nature* **2007**, *446*, 423 – 427.
[3] a) R. B. Woodward, R. Hoffmann, *Angew. Chem.* **1969**, *81*, 797 – 869; *Angew. Chem. Int. Ed. Engl.* **1969**, *8*, 781 – 853; b) R. B. Woodward, R. Hoffmann, *J. Am. Chem. Soc.* **1965**, *87*, 395 – 397.
[4] J. Ribas-Arino, M. Shiga, D. Marx, *Angew. Chem.* **2009**, *121*, 4254 – 4257; *Angew. Chem. Int. Ed.* **2009**, *48*, 4190 – 4193.
[5] M. T. Ong, J. Leiding, H. Tao, A. M. Virshup, T. J. Martinez, *J. Am. Chem. Soc.* **2009**, *131*, 6377 – 6379.
[6] S. Sakai, *J. Mol. Structure (Theochem)* **1999**, *461*, 283 – 295.
[7] J. Breulet, H. F. Schaefer III, *J. Am. Chem. Soc.* **1984**, *106*, 1221 – 1226.

[8] a) C. Bustamante, Y. R. Chemla, N. R. Forde, D. Izhaky, *Annu. Rev. Biochem.* **2004**, *73*, 705 – 748; b) E. Evans, K. Ritchie, *Biophys. J.* **1997**, *72*, 1541 – 1555.
[9] a) M. W. Schmidt, K. K. Baldridge, J. A. Boatz, S. T. Elbert, M. S. Gordon, J. H. Jensen, S. Koseki, N. Matsunaga, K. A. Nguyen, S. Su, T. L. Windus, M. Dupuis, J. A. Montgomery, *J. Comput. Chem.* **1993**, *14*, 1347 – 1363; b) M. S. Gordon, M. W. Schmidt in *Theory and Application os Computational Chemistry, the First Forty Years* (Eds.: C. E. Dykstra, G. Frenking, K. S. Kim, G. E. Scuseria), Elsevier, Amsterdam, **2005**, pp. 1167 – 1189.
[10] a) W. G. Hoover, *Phys. Rev. A* **1985**, *31*, 1695 – 1967; b) S. Nosé, *J. Chem. Phys.* **1984**, *81*, 511 – 519.

